AIAA JOURNAL
Vol. 31, No. 3, March 1993

Experimental Investigation of a Three-Dimensional Bluff-Body Wake

A. Ahmed,* M. J. Khan,† and B. Bays-Muchmore‡
Texas A&M University, College Station, Texas 77843

The flowfield behind the wavy-cylinder geometry has been examined using flow visualization, total pressure surveys, and two-component laser Doppler anemometry. The topology of the boundary-layer separation line is linked to the subsequent three-dimensional development of the mean and turbulent structures of the wake. The formation of trailing streamwise vortices behind the nodal points of separation results in a locally narrower wake, a more rapid wake velocity recovery, and suppression of the turbulence development within the separated boundary layer. The dynamic behavior of the trailing vortices suggests that vortex pairing is suppressed by the presence of an axial strain field. The Reynold stress field in the immediate wake exhibited large spanwise variations even though the wavy-cylinder geometry did not affect the spanwise spacing of the dominant foci structures on the leeward side of the cylinder or the spanwise spacing of the rib vortices located in the braid region between consecutive von Kármán vortices.

Introduction

THREE-DIMENSIONAL phenomena in fluid flow over nominally two-dimensional circular cylinder geometries have been the topic of several investigations.[1-4] Three-dimensional phenomena have also been reported in the wakes of three-dimensional application-oriented geometries, such as stranded cables.[5] In such cases, it is difficult to distinguish between the three-dimensional effects due to inherent wake instabilities and those due to the geometry. The wavy-cylinder geometry, shown in Fig. 1, is a natural three-dimensional extension of the right circular cylinder geometry, allowing parametric variation of the strength of the three-dimensionality explicitly introduced into the flowfield. Earlier we reported the surface pressure distributions and surface flow patterns for a set of wavy cylinders.[6] In this paper we explore the effects of the three-dimensional separation line topology on the development of the turbulent wake. Flow visualizations, total pressure surveys, and laser Doppler velocimetry (LDV) measurements of the mean velocity field and Reynolds stresses are presented and analyzed.

The terminology used to describe the wavy cylinders is shown in Fig. 1. The axial locations of maximum diameter are hereafter termed "geometric nodes" and the axial locations of minimum diameter are termed "geometric saddles."

Description of Experiments

Five wavy-cylinder models were used in the wind-tunnel and water-tunnel tests. These cylinders are described by the equation:

$$R_{\text{local}} = R_{\text{mean}} - A\cos(2\pi Z/\lambda)$$

For all five cylinders, R_{mean} was 31.75 mm, amplitude A was 6.35 mm, and the mean diameter D was 63.50 mm. The only difference between the cylinders was that their wavelengths λ were 50.8, 76.2, 101.6, 127.0, and 152.4 mm. Hereafter the cylinders are referred to by the appropriate value of λ/D: either 0.8, 1.2, 1.6, 2.0, or 2.4. A right circular cylinder of 59.2 mm diameter was also tested.

Total pressure surveys, using a Kiel probe, were conducted in the Texas A&M University 0.6×0.9 m (2×3 ft) low-speed wind tunnel in the wakes of the $\lambda/D = 0.8$ and 2.4 wavy cylinders at Reynolds numbers of 5 and 6.5×10^4, respectively. Flow-visualization and LDV data collection were done in the Texas A&M University 0.6×0.9 m (2×3 ft) water tunnel. The experimental setup, techniques, and LDV system are described in detail in Ref. 7.

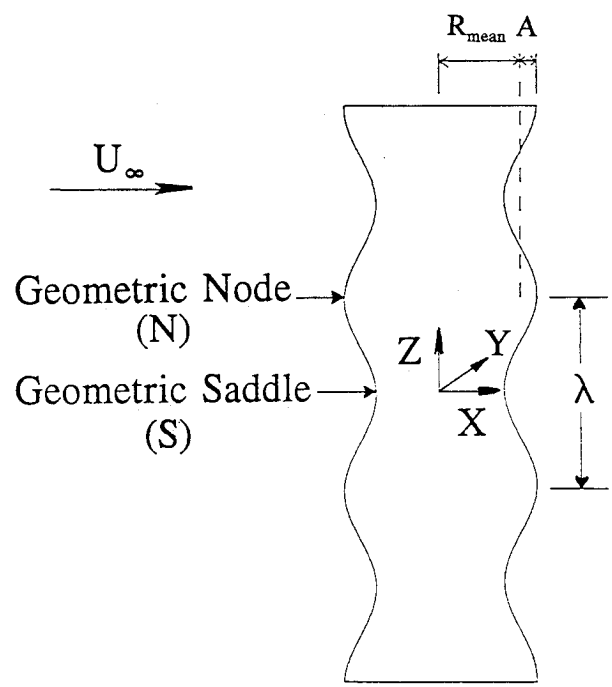

Fig. 1 Coordinate system and nomenclature of the wavy cylinder.

Received Nov. 12, 1991; presented as Paper 92-0429 at the AIAA 30th Aerospace Sciences Meeting, Reno, NV, Jan. 6-9, 1992; revision received Aug. 5, 1992; accepted for publication Aug. 5, 1992.

*Assistant Professor, Department of Aerospace Engineering. Member AIAA.

†Doctoral Candidate, Department of Aerospace Engineering. Student Member AIAA.

‡Graduate Student, Department of Aerospace Engineering; currently, Research Engineer, The Boeing Company, Seattle, WA 98124. Member AIAA.

Results and Discussion

An interpretation of the velocity field near the wavy-cylinder separation line is given in Fig. 2. A detailed discussion of the wavy-cylinder surface flowfield that creates this separation behavior is given in Ref. 6; for the current discussion, our emphasis is on the effects of the separation-line topology on the downstream wake development.

Behavior of the Separated Shear Layer

Two-dimensional slices of the wake behind the nodes and saddles obtained using the laser-light-sheet technique are given in Fig. 3 for a $\lambda/D = 1.2$ wavy cylinder at three different Reynolds numbers (5×10^3, 1×10^4, and 2×10^4). As reported by other investigators using flow visualization and hot-wire anemometry,[8,9] for a right circular cylinder at $Re = 5 \times 10^3$, the separated boundary layer develops several shear-layer vortices between the point of separation and the region where it is engulfed into the von Kármán vortex formation region. At this Reynolds number the shear-layer vortices do not amalgamate, and the shear layer can be considered transitional, not turbulent, when it is engulfed into the von Kármán vortex formation region. By $Re = 2 \times 10^4$ the combination of a higher wave number and earlier onset of shear-layer vortex formation allows the separated boundary layers to achieve what may be considered a "fully turbulent" state before they are engulfed in the von Kármán vortex formation region.

The photographs in Fig. 3 show that for the $\lambda/D = 1.2$ wavy cylinder the development of the shear layer behind the geometric saddles resembles the right-circular cylinder case. Behind the geometric nodes, where the streamwise vortices form, the wake is narrower and the rolling up of the separated boundary layer into streamwise vortices suppresses or delays the development of the shear-layer vortices. The results for the other wavy cylinders were similar.

The result of a total pressure survey behind the $\lambda/D = 0.8$ wavy cylinder at $X/D = 1.6$ and $Re = 5 \times 10^4$ are shown in Fig. 4. The shape of the total-pressure coefficient contours resemble projections of the wavy-cylinder geometry itself, but as indicated by the labels on the side axis the wake is widest behind the geometric saddles where the cylinder is narrowest and the wake is narrowest behind the geometric nodes where the cylinder is widest. The quantitative accuracy of the data in Fig. 4 is questionable due to high local flow angularity and the intrusive nature of the Kiel probe; we have presented the figure only to indicate the overall shape of the mean wake.

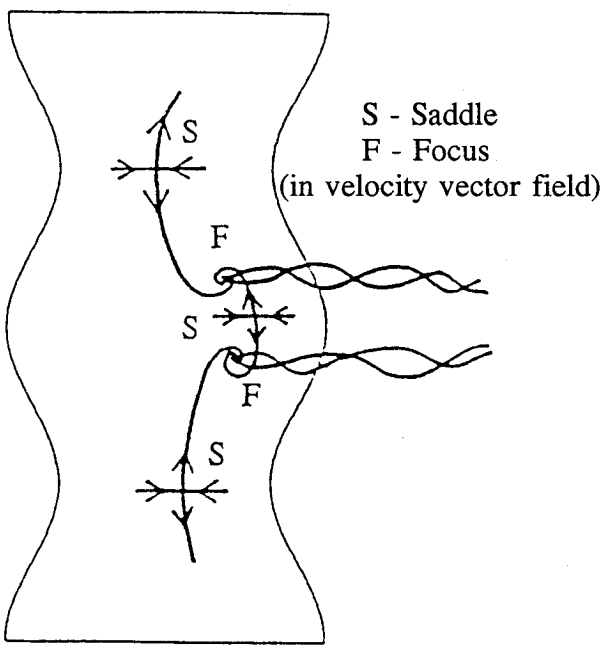

Fig. 2 Separation line topology of the wavy cylinder.

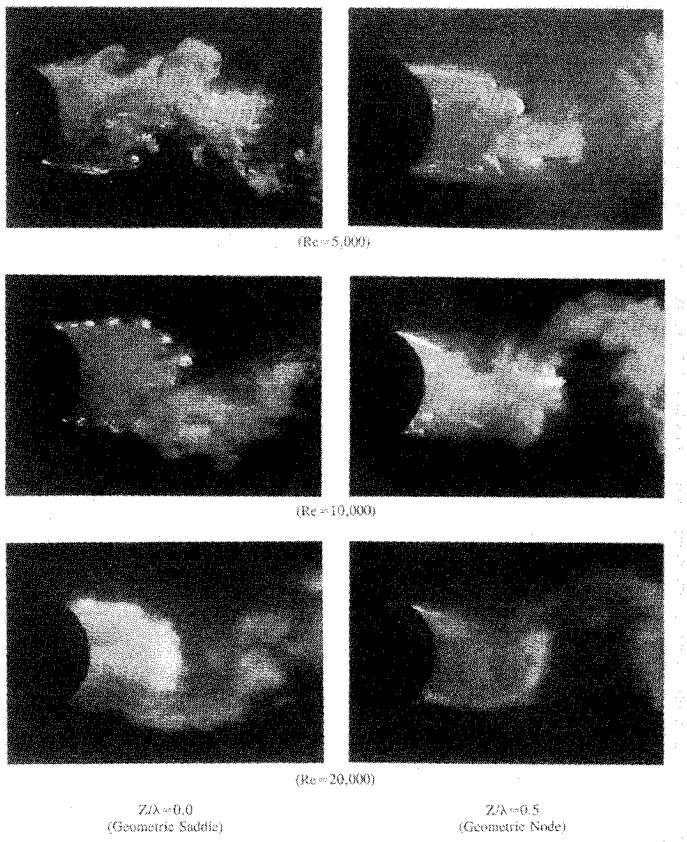

Fig. 3 Wake of a $\lambda/D = 1.2$ wavy cylinder.

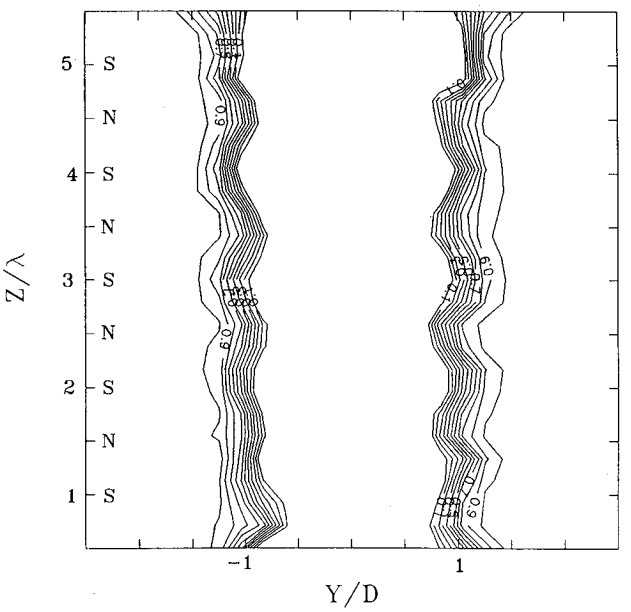

Fig. 4 Contours of constant total pressure coefficient at $X/D = 1.6$ for $\lambda/D = 0.8$ wavy cylinder at $Re = 5 \times 10^4$.

Coherent Structures and Secondary Vortices (ribs)

One purpose of the wavy-cylinder research program was to determine the sensitivity of near-wake turbulent structures to surface geometry. For the right circular cylinder the coherent structures in the immediate wake are the von Kármán vortices. Throughout the flow visualization tests these vortices were observed to maintain the same degree of spanwise coherence

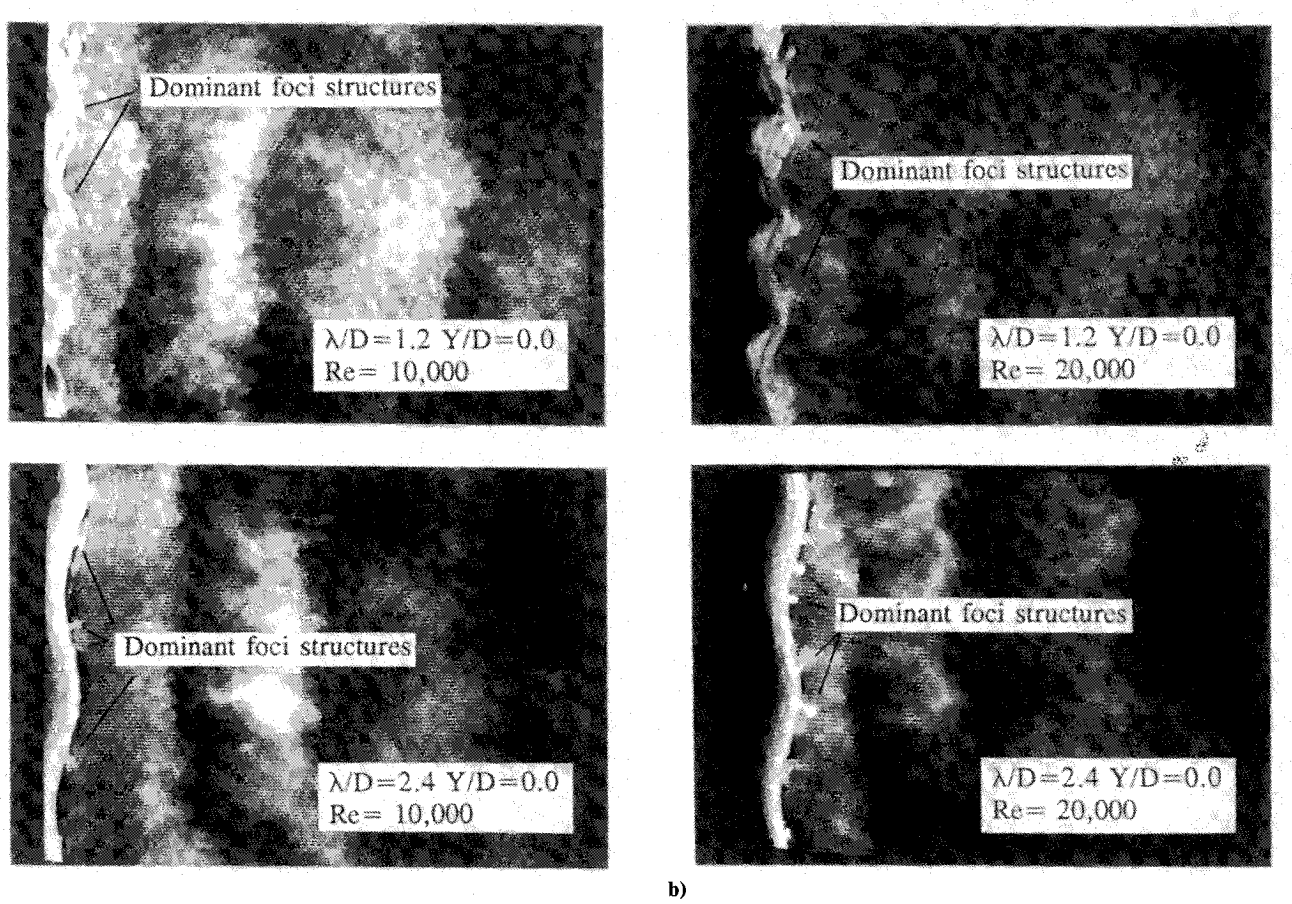

Fig. 5 Spacing of dominant foci structures and mushroom shapes (indicating pairs of ribs) behind the wavy cylinder (laser light sheet parallel to the *X-Z* plane).

behind the wavy cylinders as behind the right circular cylinder. This is not surprising since the von Kármán vortices can be attributed to an inviscid instability in the wake and the spanwise variations in mean velocity profiles (in the *X-Y* plane) are small relative to the gradients of the profiles themselves.

Streamwise vortices (hereafter termed ribs after Hussain[10]) have been reported in flow visualizations of low Reynolds number cylinder wakes ($Re = 1.8 \times 10^2$ to 1×10^3)[11-15] and arrays of *X*-film probes have detected vorticity patterns consistent with the existence of ribs in the turbulent wake 20 diameters downstream of a cylinder at $Re = 1.3 \times 10^4$. Recently, we reported the existence of ribs in the immediate wakes of right circular cylinders over a range of Reynolds numbers from 3.3×10^2 to 2.1×10^4 and linked their initial creation with the existence of dominant foci structures present in a secondary separation line on the leeward side of the cylinder.[6] The secondary turbulence structures intuitively seem likely to be affected by modifications to the cylinder geometry: a common explanation for the creation of ribs in the braid region between coherent structures is amplification of deformations of the coherent structures themselves.

Figure 5 shows side views of the wakes of two of the cylinders tested (the $\lambda/D = 1.2$ and 2.4 wavy cylinders) with the laser light sheet positioned along the wake centerline for $Re = 1$ and 2×10^4. The existence of the counter-rotating rib pairs are identifiable by the mushroom-shaped regions of dye evident on the upstream-facing sides of the von Kármán vortices. The dominant foci structures, visible as dye erupting from the surface, are present on each of the cylinders, and the spacing of the rib pairs is approximately one cylinder diameter in each case, independent of cylinder waviness. For all wavy cylinders tested, the spanwise locations of the rib pairs were uncorrelated with the surface geometry. Based on the consistency of the spanwise spacing of the ribs observed in the wake of right circular cylinders over a wide range of Reynolds numbers, we concluded that the structure of the separated boundary layer had little influence on the rib formation. The current results support this conclusion: even when the separated boundary layer contains significant spanwise distortions, the spanwise spacing and spatial locations of the ribs are unaffected.

Vortex Pairing

The shorter wavelength cylinders clearly exhibited two counter-rotating vortices behind each geometric node, but these vortices were observed to pair helically in a short distance downstream. For $Re = 5 \times 10^3$, a low-energy fluid region existed between the trailing edge of the cylinders and the forming von Kármán vortices. The size of this region decreased as Reynolds number increased, and by $Re = 2 \times 10^4$ the von Kármán vortices formed directly behind the cylinder. The pairing behavior of the trailing vortex pairs also changed over this range of Reynolds numbers. For $Re = 5 \times 10^3$ the vortices paired quickly and tended to drift spanwise; for $Re = 2 \times 10^4$ they were less likely to pair immediately and remained more spatially fixed. This same behavioral difference was also observed over the period of each von Kármán shedding cycle at a fixed Reynolds number. Figure 6 shows a *Y-Z* planar slice of the wake just behind the $\lambda/D = 1.2$ wavy cylinder at $Re = 1 \times 10^5$. The upper left corner of Fig. 6a shows a pair of counter-rotating vortices that have nearly merged (or amalgamated or paired). Moments later the flow pattern had changed to that shown in Fig. 6b, with the vortices vertically aligned and oriented so as to induce outer fluid to flow toward the wake centerline at the node. The pairing of the vortices is suppressed during phases of the von Kármán shedding when the separated fluid is accelerated by the forming vortex downstream, and hence the streamwise trailing

a) b)

Fig. 6 Longitudinal vortices in the wake of $\lambda/D = 1.2$ wavy cylinder viewing upstream (laser light sheet in Y-Z plane directly behind the cylinder). Note vortex structure at upper left corner of each photograph.

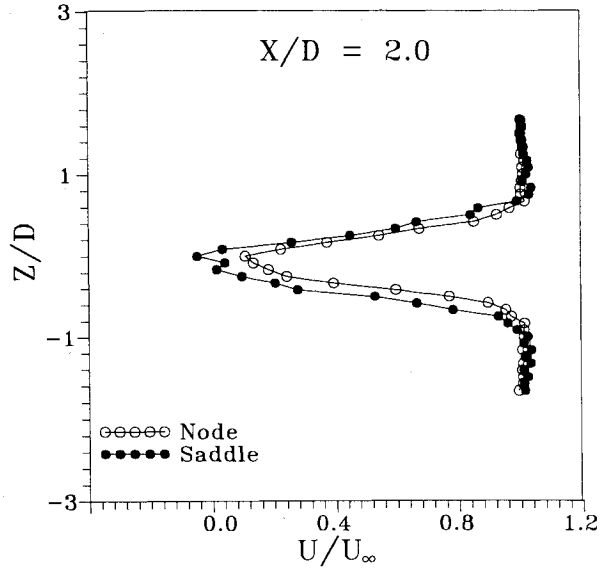

Fig. 7 Mean velocity profiles in the wake of $\lambda/D = 1.2$ wavy cylinder.

vortices are subjected to an axial strain field. This acceleration is greater at the higher Reynolds number when the von Kármán vortices form closer to the point of separation. Mean velocity profiles obtained at $X/D = 2.0$ given in Fig. 7 show that the wake width and maximum velocity defect is greater behind the saddle than behind the node. The nondimensional Reynolds stresses are presented in Fig. 8.

The u'^2/U_∞^2 values shown in Fig. 8a are greater behind the geometric saddle than behind the geometric node. This can be attributed to a combination of the following:

1) The separated boundary layers behind the saddles contain a higher level of shear-layer turbulence (see Fig. 3).

2) The von Kármán vortices behind the saddles have greater total circulation since some of the vorticity of the separated boundary layer behind the nodes is entrained by the streamwise vortices.

The v'^2/U_∞^2 and $u'v'/U_\infty^2$ values behind the geometric node shown in Figs. 8b and 8c have greater peak values near the center of the wake but lower values near the edge of the wake compared to the values behind the geometric saddle. Since the wake behind the geometric saddle is wider it is not surprising that the turbulence levels also extend further from

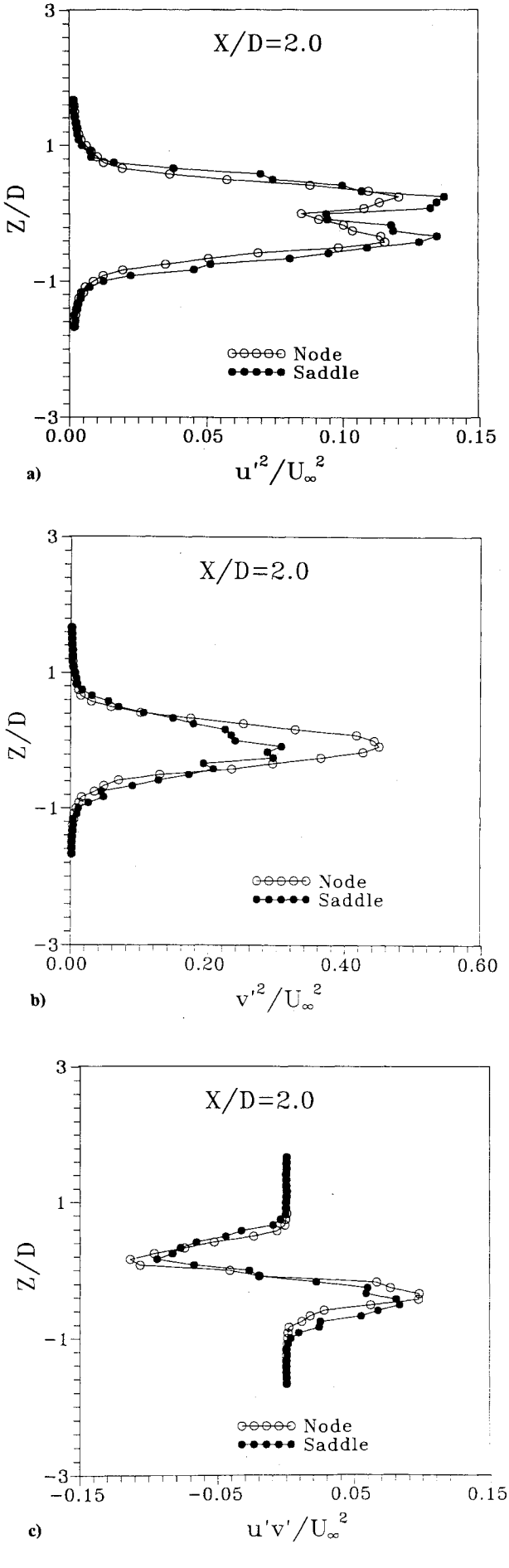

Fig. 8 Reynolds stresses in the wake of $\lambda/D = 1.2$ wavy cylinder.

the wake centerline. The higher peak values may be due to a combination of: 1) induced velocities from the streamwise trailing vortices and 2) greater induced velocities near the wake centerline from more concentrated (smaller diameter) von Kármán vortices.

Conclusions

1) The primary significance of the three-dimensionality of the wavy-cylinder separation lines is that streamwise vortices form near the nodal points of separation.

2) The turbulence structures in the separated boundary layer behind the saddle points of separation develop in a manner similar to those in a simple mixing layer. Behind the nodal points of separation, the "rolling up" of the separated boundary layer delays or suppresses the development of the shear-layer turbulence.

3) The formation of the trailing vortices results in a wavy-cylinder wake that is narrowest behind the geometric nodes (where the cylinder is widest) and widest behind the geometric saddles (where the cylinder is narrowest).

4) The spanwise spacing of the dominant foci structures on the leeward side of the cylinders and the spanwise spacing of the rib vortices were unaffected by the cylinder spanwise waviness.

5) The dynamic behavior of the trailing vortical structures indicated that the counter-rotating vortices tended to pair and drift spanwise in the absence of a longitudinal strain field, whereas the presence of such a strain field suppressed vortex pairing and stabilized them spatially.

6) The wake region immediately behind the geometric nodes, near the streamwise vortices, contains lower streamwise normal stresses but higher transverse normal and shear stresses.

References

[1]Dallmann, U., and Schewe, G., "On Topological Changes of Separating Flow Structures at Transition Reynolds Numbers," AIAA Paper 87-1266, 1987.

[2]Hayakawa, M., and Hussain, F. "Three-Dimensionality in a Plane Turbulent Wake," *Journal of Fluid Mechanics,* Vol. 206, Sept. 1989, pp. 375–404.

[3]Williamson, C. H. K., "Three-Dimensional Aspects and Transition of the Wake of a Circular Cylinder," *Proceedings of the 7th Symposium on Turbulent Shear Flows,* Springer-Verlag, Berlin, 1991, pp. 173–194.

[4]Bays-Muchmore, B., and Ahmed, A., "On Streamwise Vortices in the Turbulent Wakes of Cylinders," *Bulletin of the American Physical Society,* Vol. 36, No. 10, 1991, p. 2620.

[5]Nebres, J., Batill, S., and Nelson, R., "Wake Studies on Yawed, Stranded Cables," *Low Reynolds Number Aerodynamics, Lecture Notes in Engineering 54,* edited by T. Mueller, Springer-Verlag, Berlin, Germany, pp. 433–446.

[6]Ahmed, A., and Bays-Muchmore, B., "Transverse Flow over a Wavy Cylinder," *Physics of Fluids A,* Vol. 4, No. 9, 1992, pp. 1959–1967.

[7]Bays-Muchmore, B., "An Experimental Investigation of the Surface Flow and Wake Dynamics Associated with Transverse Flow over Wavy Cylinders," Ph.D. Dissertation, Texas A&M Univ., College Station, TX, Aug. 1991.

[8]Wei, T., and Smith, C. R., "Secondary Vortices in the Wake of Circular Cylinder," *Journal of Fluid Mechanics,* Vol. 169, Aug. 1986, pp. 513–533.

[9]Kourta, A., Boisson, H. C., Chassaing, P., and Minh, H., "Nonlinear Interaction and the Transition to Turbulence in the Wake of a Circular Cylinder," *Journal of Fluid Mechanics,* Vol. 181, 1987, pp. 141–161.

[10]Hussain, A. K. M. F., "Coherent Structures and Turbulence," *Journal of Fluid Mechanics,* Vol. 173, 1986, pp. 303–356.

[11]Hama, F. R., "Three-Dimensional Vortex Patterns Behind a Circular Cylinder," *Journal of Aeronautical Sciences,* Vol. 24, No. 2, 1957, pp. 156–164.

[12]Gerrard, J. H., "The Three-Dimensional Structure of the Wake of a Circular Cylinder," *Journal of Fluid Mechanics,* Vol. 25, 1966, pp. 143–164.

[13]Taneda, S., "Irregular Flows," *Sadhana,* Vol. 10, No. 8, Part 3/4, 1987, pp. 349–375.

[14]Williamson, C. H. K., "The Existence of Two Stages in the Transition to Three-Dimensionality of a Cylinder Wake," *Physics of Fluids,* Vol. 31, No. 11, 1988, pp. 3165–3168.

[15]Williamson, C. H. K., and Roshko, A., "Measurements of Base Pressure in the Wake of a Cylinder at Low Reynolds Numbers," *Zeitschrift Für Flugwissenschaften und Weltraumforschung,* Vol. 14, No. 1/2, 1990, pp. 38–46.